Journal of Applied Pharmaceutical Science Vol. 13(07), pp 258-269, July, 2023
Available online at http://www.japsonline.com
DOI: 10.7324/JAPS.2023.135443
ISSN 2231-3354

Cholate-based nano emulgel of 1,1-dimethylbiguanide can diminish the liver damage in NAFLD induced by high-fat diet

Heba F. Salem[1,2], Mohammed M. Nafady[3*], Adel A. Ali[1], Nermeen M. Khalil[3], Amani A. Elsisi[1]

[1]Department of Pharmaceutics & Industrial Pharmacy, Faculty of Pharmacy, Beni-Suef University, Beni-Suef, Egypt.
[2]6 October Technological University, Cairo, Egypt.
[3]Department of Pharmaceutics, Faculty of Pharmacy, Nahda University Beni-Suef, Egypt.

ARTICLE INFO

Received on: 31/01/2023
Accepted on: 10/05/2023
Available Online: 04/07/2023

Key words:
Metformin HCl, cholate-based nanovesicles emulgel, rheology study, tumor necrosis factor-alpha, liver targeting.

ABSTRACT

NAFLD (nonalcoholic fatty liver disease) is a widely spread disease that, till now, has no approved therapy, and enhancing the patient's case depends only on lifestyle modification. In this research, cholate-based 1,1-dimethylbiguanide (metformin HCl) was incorporated into an emulgel to investigate its transdermal effect in treating NAFLD. metformin HCl cholate-based nanovesicles were prepared with the solvent vaporization technique. Vesicles are imaged by transmission electron microscope to ensure the vesicles formation, and their charge is detected to inspect their stability. The vesicles were then incorporated into a prepared Carbopol emulgel and then were characterized. Finally, an *in vivo* study on balb-c mice was performed to inspect its effect in treating NAFLD topically. The resulting vesicles were stable, sphere-shaped, and nonaggregated with a coarse surface. In addition, prepared emulgel was found clear and homogenous with general characteristics suitable for skin application. Furthermore, the rheology study showed a thixotropic performance. Finally, the *in vivo* study revealed an overall enhancement confirming the liver targeting ability of cholate-based bile salts. Cholate-based nanovesicles emulgel of metformin HCl is an approach for an acceptable level of evidence of effective transdermal treatment of NAFLD.

INTRODUCTION

NAFLD (nonalcoholic fatty liver disease) is considered a comprehensive world health problem nowadays (Bellentani *et al*., 2010). It includes fatty liver and steatohepatitis starting from liver fatty vacuoles and fibrosis leading to hepatic cancer (Hadizadeh *et al*., 2017). Until now, no known therapy has been approved for treating NASH (nonalcoholic steatohepatitis) (Sporea *et al*., 2018). NAFLD *in vivo* study should be done on a suitable animal model that resembles NAFLD pathogenesis in humans and is caused by the same risk factors (obesity, fatty diet, high sugars, and insulin resistance) (Hadizadeh *et al*., 2017). NAFLD pathogenesis comprises abnormality in liver enzymes and lipid profile serum samples, tumor necrosis factor alpha (TNF-α) elevation, and fat vacuolation in liver histology with mild to severe fibrosis (Hadizadeh *et al*., 2017; Sporea *et al*., 2018)

Metformin HCl (C4H12ClN5; 3-(diaminomethylidene)-1, 1-dimethylguanidine; hydrochloride). It is the hydrochloride salt of biguanide antidiabetics with antihyperglycemic activity. Only 50% of an orally administered dose is absorbed from the gut. Therefore, metformin is a biopharmaceutics class III. Furthermore, it helps to reduce low-density lipoprotein (LDL), cholesterol, and triglycerides (TG) levels. Metformin is not metabolized and is excreted by the renal. Its molecular weight is approximately 165, and its water miscible. Metformin HCl is the drug of choice in treating diabetes mellitus type II (Cicero *et al*., 2012). Also, recent studies have shown its valuable effect on other diseases such as obesity, cancer, circulatory diseases, and fatty liver (Salem *et al*., 2022) (Green *et al*., 2019; Li *et al*., 2013).

Different oral formulations were studied for metformin HCl (Ng and Gupta, 2020), for instance, traditional tablets,

*Corresponding Author
Mohammed M. Nafady, Department of Pharmaceutics, Faculty of Pharmacy, Nahda University Beni-Suef, Beni-Suef, Egypt.
E-mail: mohammed.nafady @ yahoo.com

sustained-release tablets (Basak *et al*., 2008), and floatable gastroretentive tablets (Basak *et al*., 2007). Though severe gastritis and poor oral absorption are the significant drawbacks of metformin oral administration methods, (Jain and Gupta, 2009) more studies lead to the possibility of topical delivery of metformin HCl through advanced nanodelivery systems (Salem *et al*., 2022). Metformin is known to enhance insulin resistance besides its TNF-α suppression ability, so that it can be used in treating NAFLD.

Cholate-based nanovesicles are spherical bilayered bile salts-based vesicles that are 5–200 nm in size and can be uni- or multilamellar. In general, cholate-based nanovesicles consist of two layers; the inner layer consists of hydrophilic drugs and (or) antigens, and the outer layer consists of bile salts and (or) hydrophobic drugs. Materials used in the formulation of cholate-based nanovesicles encompass mainly nonionic surfactants and bile salts; lipids such as phosphatidylcholine and cholesterol are also included. It involves nonionic surfactants and exhibits a better quality of transdermal delivery than other nanovesicles (Al-Mahallawi *et al*., 2015). Bile salts produce extremely stable vesicles for transdermal distribution by acting as electrostatic stabilizers and edge activators with fluidizing effects (El Zaafarany *et al*., 2010). Cholate-based nanovesicles can be prepared by the solvent vaporization method (Al-Mahallawi *et al*., 2015).Cholate-based nanovesicles are advanced vesicles (Ahmed *et al*., 2020) known as liver targeting molecules formed mainly from bile salts and surfactants (Al-Mahallawi *et al*., 2015). Recently, it was studied to enhance the permeation of metformin through the skin stratum corneum layer and showed stunning results (Salem *et al*., 2022). So incorporating of cholate-based nanovesicles into an emulgel could be an advanced delivery system that gives a thixotropic behavior with a nongreasy emollient application (Alexander *et al*., 2013).

The *in vivo* study of NAFLD should be done on a suitable animal model that resembles NAFLD pathogenesis in humans and is caused by the same risk factors (Hadizadeh *et al*., 2017). Therefore, balb-c mice were chosen as animal models for NAFLD. However, it is known to resist the change in body weight (Kim *et al*., 2011; Nishikawa *et al*., 2007). It reflexes a good pathology indication in serum analysis, hepatic histology, and liver weight (Hadizadeh *et al*., 2017; Rahmadi *et al*., 2021; Xie *et al*., 2015).

Aberration of ALT (transaminases alanine aminotransferase) and AST (aspartate aminotransferase) values is frequently associated with NAFLD. Through around 60 transamination reactions, only ALT and AST are clinically significant. In copious studies of NAFLD patients, raised levels of aminotransferases and diabetes have been ascertained as steadfast predictors of fibrosis in patients with a risk of progressing to advanced fibrosis (Harrison *et al*., 2003).

TNF-α has an indispensable effect on the development of NAFLD due to its proinflammatory influence (Hadizadeh *et al*., 2017; Jovinge *et al*., 1998). In addition, it provokes hepatocytes apoptosis and proliferation causing liver fibrosis (Galle, 1997; Yang and Seki, 2015). Moreover, TNF-α increases the TG serum concentrations (Jovinge *et al*., 1998) and reduces serum HDL-c levels and insulin sensitivity (Tacer *et al*., 2007). In NAFLD, the serum levels of TNF-α raises, so standardization of its concentration improves insulin sensitivity and NAFLD (Ajmal *et al*., 2014; Hadizadeh *et al*., 2017).

In this research, metformin cholate-based nanovesicles emulgel was prepared and characterized as an approach for acceptable level of evidence of effective transdermal treatment of NAFLD in balb-c mice through different mechanisms avoiding the drastic side effects of metformin.

MATERIALS AND METHODS

Metformin HCl was kindly provided by Cid Pharmaceutical Co. (Assuit, Egypt). Span 60 (S60) (sorbitan monostearate), Span 80 (S80) (Sorbitan monooleate), and Tween 80 (polysorbate 80) are purchased from Oxford Laboratory (El-Nasr Pharmaceutical Chemicals Co., Sohag, Egypt). Sodium deoxycholate (SDC) is purchased from Acros Organics (El-Nasr Pharmaceutical Chemicals Co., Sohag, Egypt). Cholesterol is purchased from Sigma Aldrich, Saint Louis, MO. Methanol and methylene chloride ADWIC are purchased from El-Nasr Pharmaceutical Chemicals Co., Sohag, Egypt. Carbopol 940 and polyethylene glycol (PEG 400) were purchased from LOBA Chemie, Mumbai, India. Dimethyl sulfoxide (DMS), triethanolamine, and ethanol were obtained from El-Nasr Pharmaceutical Chemicals Co., Cairo, Egypt. All reagents were of analytical grade and were commercially available.

Standard calibration curve

Stock solution (1 mg/ml) of metformin HCl dissolved in phosphate citrate buffer pH 4 was used to establish a standard calibration curve, and serial dilutions (1 to 8 µg/ml) were prepared. Metformin HCl was analyzed using a UV spectrophotometer at λ max = 233 nm. The absorbances were plotted against the concentrations, and the linear regression equation was calculated.

Formulation of metformin HCl cholate-based bile salts

Metformin HCl cholate-based nanovesicles were formulated through the solvent vaporization method with slight modification (Salem *et al*., 2022). Concisely, metformin HCl (600 mg) and cholesterol (14 mg) were dissolved in a methanol-to-methylene-chloride (1:2) mixture after addition of 130 mg of span 60 (as a surfactant) and 8 mg of SDC (as an edge activator). The solvents were then completely evaporated by continuous agitation on a magnetic stirrer (IKA, C-MAG HS 7 digital, Germany) at 60°C. The resulting residue was then hydrated with phosphate citrate buffer pH 4 to obtain the cholate-based nanovesicles suspension. Phosphate citrate buffer pH 4 was used because of the metformin HCl tendency to be more soluble in acidic media, while the pH of the skin ranges from 4 to 6.(El-Menshawe *et al*., 2018)

Morphology of metformin HCl cholate-based nanovesicles by TEM (Transmission electron microscope)

The vesicles morphology was reconnoitered using high-resolution TEM (JEOL Co., JEM-1400; Japan) (negative stain technique) to ensure the successful formation of the cholate-based bile salts. First, the formulation was suitably diluted with distilled water; then, a drip was put above a carbon-coated copper grating and stained with a phosphotungstic dye at 160 KV fast-tracking voltage (El-Menshawe *et al*., 2018).

Zeta size and potential of metformin HCl cholate-based bile salts

The zeta size and potential of the prepared formulation (diluted with 4 ml distilled water) were detected using the dynamic

light-scattering technique applied by the zeta seizer (Malvern ZetaSizer3000, UK) with a fixed angle of 90° at room temperature (25°C) (El-Menshawe *et al*., 2018).

Preparation of metformin HCl cholate-based nanovesicles emulgel

Carbopol 940 (1% *w*/*w*) as a gelling agent was kept overnight in water at 4°C, then 15% *w*/*v* PEG-400 (polyethylene glycol-400) was added to get a homogeneous gel. The emulsion (*o*/*w* type) was prepared by adding the oily phase continuously with stirring to the aqueous phase; span 80 was dissolved in castor oil to prepare the emulsion oil phase, while Tween 80 was dissolved in purified water to prepare the aqueous phase. The oil and aqueous phases of the emulsion were separately heated to 75°C and allowed to cool to room temperature. The emulsion and the carbopol gel were mixed in a 1:1 ratio with mild rousing to obtain the emulgel and then triethanolamine (1%) was dropped to maintain the pH. Finally, a calculated weight of metformin HCl cholate-based nanovesicles equivalent to 600 mg of metformin HCl was incorporated into the obtained emulgel (Mohamed *et al*., 2019).

Characterization of metformin HCl cholate-based nanovesicles emulgel

Clarity and homogeneity of metformin HCl cholate-based nanovesicles emulgel

The clarity and homogeneity of the prepared cholate-based nanovesicles emulgel were evaluated visually against white and black backgrounds to evaluate the manifestation of any aggregation or turbidity. The formulation was stored at room temperature (25°C) and reevaluated after 15 days.

The pH of metformin HCl cholate-based nanovesicles emulgel

The pH meter (Jenway 3510 pH meter; Staffordshire, UK) was used to determine the cholate-based nanovesicles emulgel pH. Briefly, 1 ml of the prepared cholate-based nanovesicles emulgel was suitably diluted with distilled water (10 ml) and allowed to equilibrate before dipping the pH meter probe (Vani *et al*., 2018). The pH measurements were implemented in triplicate, and the mean was calculated. The formulation was reevaluated after 15 days of storing at room temperature (25°C).

Rheology study of metformin HCl cholate-based nanovesicles emulgel

The viscosity of the prepared emulgel was determined over a wide range of speeds (10–100 rpm) to inspect its rheology behavior using Brookfield viscometer (HBDV-III Ultra; Brookfield Engineering Laboratories, Stoughton, MA) with a suitable spindle (CP 40 model HB). The gap between every two consecutive measurements was 30 seconds and the test was done at room temperature (25°C) (Salem *et al*., 2021). The hysteresis loops and the grade of pseudoplasticity (Farrow's constant) were determined using the trapezoidal rule. Then, the area under the down curve was subtracted from the total area under the curve to attain the hysteresis loop area. Farrow's equation (Eq. 1) was applied to study the flow performance of the gel base.,

$$\text{Log } G = N \text{ Log } F - \text{Log}\eta \text{ , } (1)$$

where G is the shear rate (second^{-1}), F is the shear stress (dyne/cm^2), η is the viscosity (cP), and N is Farrow's constant.

Spreadability of metformin HCl cholate-based nanovesicles emulgel

The formulation spreadability was determined by adding 0.5 g of the prepared metformin HCl cholate-based nanovesicles emulgel between two glass slides with known dimensions (5 × 5 cm). The sample was placed on a premarked circle with a known diameter (1 cm), and the diameter increasing (spreading area) was determined after adding a standard load after 1 minute. The diameter of the spread circle was determined (Abdallah *et al*., 2021).

Extrudability of metformin HCl cholate-based nanovesicles emulgel

The extrudability of the prepared formulation was detected by calculating the amount of emulgel extruded from a lacquered aluminum portable tube. The weight of (g) required to extrude about 0.5 cm strip of gel within 10 seconds was documented. Extrudability is directly proportional to the amount of emulgel extruded. Therefore, the extrudability was determined by dividing the load weight (g) by the area (cm^2).

Drug content determination of metformin HCl cholate-based nanovesicles emulgel

One gram of the prepared cholate-based nanovesicles emulgel formulation was transferred to a 100 ml volumetric flask and diluted with phosphate citrate buffer (pH 4) to 100 ml and then allowed to dissolve in a bath sonicator. After complete dissolving, 1 ml of the prepared solution was withdrawn and rediluted to 10 ml with phosphate citrate buffer (pH 4). The sample solution was filtered and then scanned on a UV spectrophotometer at λ 233 nm against phosphate citrate buffer pH 4 as a blank, and the absorbance was detected. Drug content was calculated from the calibration curve equation (Eq. 2):

$$y = 0.112x. \quad (2)$$

***In vivo* study**

Experimental animals and ethical approval

Thirty male balb-c mice (25 ± 5 g) aged 6 weeks were obtained from the Animal Facility of Nahda University in Beni Suef, Egypt. The mice were divided into six groups (n = 5), housed in separate cages, and maintained on 60% (high-fat diet) of standard forage mixed with 4% milk powder and water ad libitum barring the normal (undiseased) group that allowed to access a standard forage. Mice were kept at room temperature maintained at 24°C ± 2°C and 12 hours light (6:00 to 18:00 hours) and dark (18:00–6:00 hours) cycles approximately (El-Menshawe *et al*., 2018). The *in vivo* study protocol was done as stated by the guidelines consented by the Pharmacology and Toxicology Department, Faculty of Pharmacy at Beni Suef University, Egypt. In addition, it was based on the National Institutes of Health Guide for Care and Use of Laboratory Animals recommendations (publication no. 85–23, revised 1985) (Albash *et al*., 2019; El-Menshawe *et al*., 2018). The animal protocol was approved by BSU-IACUC reviewers with approval number 022–351.

Experimental protocol

The six main groups of mice (n = 5) were classified as the following: Group I, control diseased; Group II, treated with plain

emulgel; Group III, treated with metformin HCl emulgel; Group IV, treated with metformin HCl cholate-based nanovesicles emulgel; Group V, treated with metformin HCl cholate-based nanovesicles emulgel including DMS as a penetration enhancer (2% *w/v*) and Group VI as a normal control. Mice's abdominal skin area (3 cm^2) was shaved using a razor (Wu *et al*., 2009) and then groups (II-V) were treated topically (according to each group) once daily for 1 month (El-Menshawe *et al*., 2018; Picchi *et al*., 2011; Popescu *et al*., 2013). Statistics was determined using Graph Pad Prism edition 6.0 for Windows, Graph Pad Software (San Diego, CA).

Measurement of food intake

The amount of mice food intake was estimated weekly by subtracting the left-over feed from the total weight of the feed given throughout the week for each group. Then, the total average food intake per month was calculated (El-Menshawe *et al*., 2018).

Measurement of average body weight

Mice's body weight was determined using Mettler balance (Toledo Type BD6000, GmbH; Greifensee, Switzerland) at the finale of the experiment (after 1 month). The amount of weight gain was computed by subtracting the average body weight at the finale of the trial from the average body weight on day 1 for each group. The percentage of weight change was calculated from the following equation (Eq. 3) (El-Menshawe *et al*., 2018):.

$$\text{Weight change \%} = \{ (\text{Amount of weight gain after one1 month}) / (\text{body weight on day 1}) \} \times 100\ \%. \quad (3)$$

Blood collection and biochemical assays

Mice fasted overnight and then blood samples were amassed from the retro-orbital plexus vein under inhaled diethyl ether anesthesia. Samples were centrifuged via laboratory centrifuge (Model SM 902B, Surgifriend Medicals, England, UK) at 10,000× g for 20 minutes; then, the supernatant serum was seceded and transferred immediately to Eppendorf tubes (Tan *et al*., 2014).The lipid profile data (cholesterol, TG) and HDL-c (high-density lipoprotein) were evaluated from the serum samples analysis, while the Friedewald and Iranian LDL-c (low-density lipoprotein) were calculated using Equations 4 and 5 (Nauck *et al*., 2002), respectively. In addition, the VLDL-c (very-low-density lipoprotein) was determined by subtracting the sum of HDL-c and LDL-c from the total cholesterol (TC). The coronary risk index (CRI = TG/HDL-c) and the atherogenic index (AI =LDL- c/ HDL-c) were also determined (Kwon *et al*., 2003)

$$\text{LDL-c} = [\text{TC} - (\text{HDL-c} + (\text{TG}/5))] \quad (4)$$

$$\text{LDL-c (Iranian)} = [((\text{TC}/1.19) + (\text{TG}/1.19) - ((\text{HDL-c})/1.1)) - 38] \quad (5)$$

The serum samples were analyzed for fasting glucose and insulin content. HOMA-IR (homeostatic model assessment for insulin resistance) was calculated as)HOMA-IR= (insulin*glucose)/405 ((Cutfield *et al*., 2003; Majid *et al*., 2017), while quantitative insulin sensitivity check index () was determined using Equation 6 (Cutfield *et al*., 2003) to evaluate the insulin resistance ability of the experimental mice.

$$\text{QUICKI} = (1/(\log \text{glucose} + \log \text{insulin})) \quad (6)$$

The liver enzymes and AST and ALT levels were determined in addition to TNF-α for all the mice by analyzing the serum samples to help diagnosing NAFLD (Neuman *et al*., 2014; Obika and Noguchi, 2011).

Hepatic weight and morphology

Mice were slew under inhaled diethyl ether anesthesia by cervical displacement at the end of the trial. Mice's livers were dissected, weighed, and then fixed in a 10% formalin/ saline solution. After that, samples were sectioned, entrenched in paraffin, and then stained with hematoxylin and eosin for histological evaluation (magnification × 100) (Tag, 2015).

RESULTS Standard calibration curve

The standard calibration curve of metformin HCl in the buffer solution (pH 4) displayed a linear relationship between the drug concentration and the UV absorption over all the concentration ranges (1–8 µg/ml), consistent with Beer-Lambert law. The regression equation and the coefficient of determination (R^2) are exemplified in Figure1.

Morphology of metformin HCl cholate-based nanovesicles by TEM

The vesicles appeared sphere-shaped and self-closed. The particles' surface was coarse, and no agglomeration was noticed (Fig. 2).

Zeta size and potential of metformin HCl cholate-based nanovesicles

The zeta size of the prepared cholate-based nanovesicles formulation was 235 ± 2.7 nm while zeta potential was found (−40 ± 5.54 mV) (Fig. 3).

Characterization of metformin HCl cholate-based nanovesicles emulgel

Clarity, homogeneity, and pH of metformin HCl cholate-based nanovesicles emulgel

The cholate-based nanovesicles emulgel of metformin HCl was clear, white, and homogenous even after storage for 15 days at room temperature (25°C); it showed no change in clarity or homogeneity. The pH detected was 4 (within the normal skin physiological range).

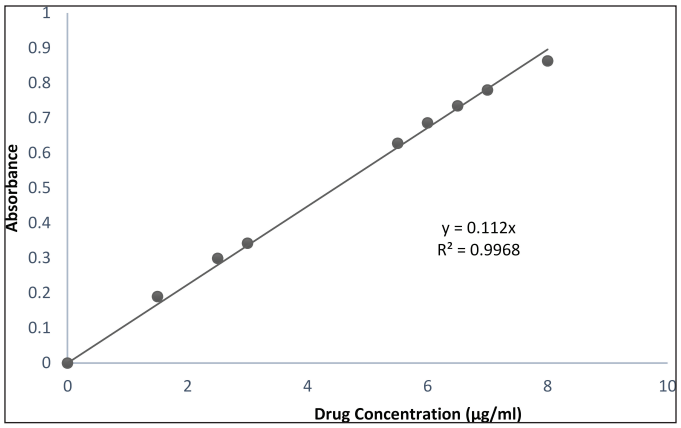

Figure 1. Standard calibration curve of metformin HCl buffer solution (pH 4).

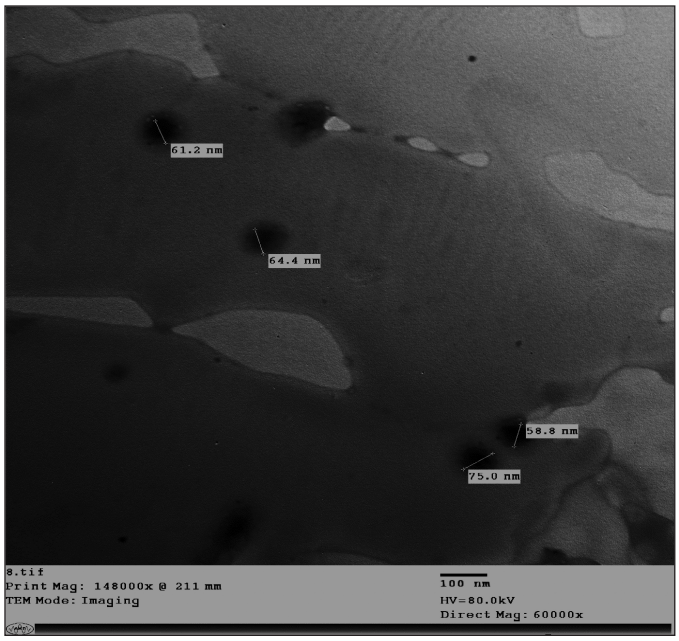

Figure 2. TEM of the prepared metformin HCl cholate-based nanovesicles.

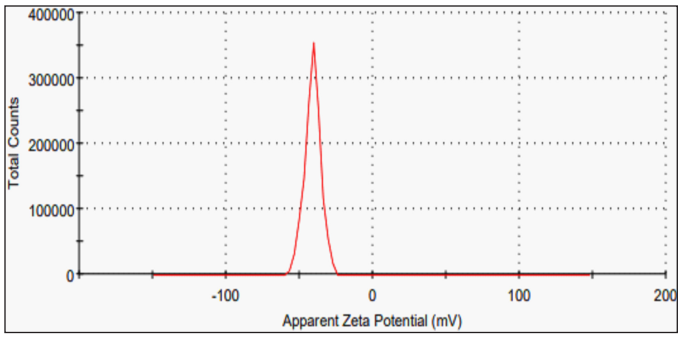

Figure 3. Zeta potential of the prepared metformin HCl cholate-based nanovesicles.

Rheology study of metformin HCl cholate-based nanovesicles emulgel

The cholate-based nanovesicles emulgel of metformin HCl showed a perfect pseudoplastic thixotropic behavior (Fig. 4a and b). In Figure 4c, by plotting log viscosity versus the log of the shear rate, this increased the rate of shear yielded in decreasing the viscosity and vice versa (inverse relationship). The hysteresis loop (the area fenced between the up and down curve) was almost negligible. The rheology parameters of the formulation are clarified in Table 1.

Spreadability of metformin HCl cholate-based nanovesicles emulgel

The spreadability of metformin HCl cholate-based nanovesicles emulgel was 3.65 ± 0.5 gcm^{S-1}.

Extrudability of metformin HCl cholate-based nanovesicles emulgel

The extrusion conduct of the prepared emulgel formulation was 5.7 ± 0.31 g/cm^2.

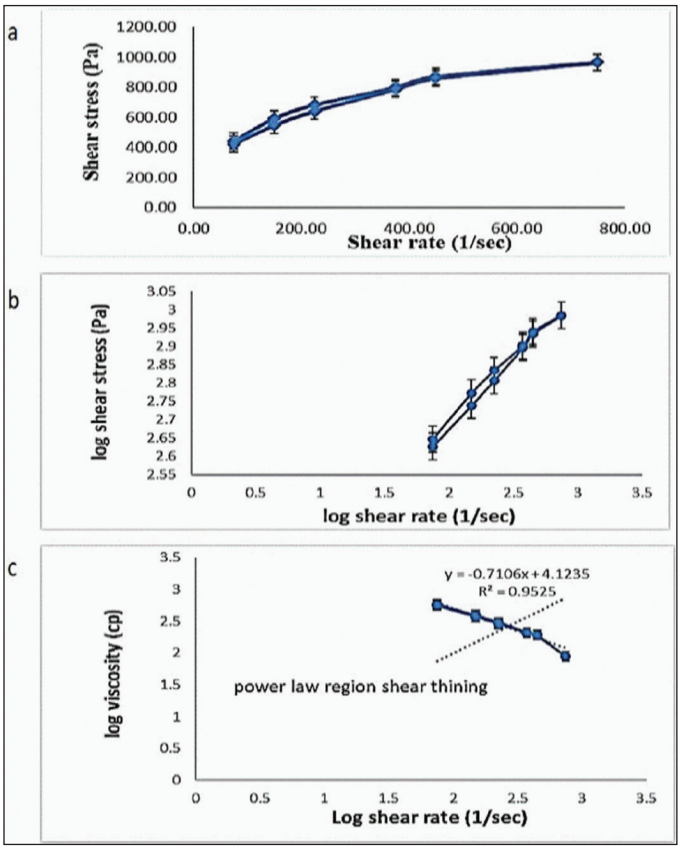

Figure 4. Rheogram of the prepared metformin HCl cholate-based nanovesicles emulgel (a) showing its thixotropic behavior (b) and the power law region shear thinning (c).

Drug content determination of metformin HCl cholate-based nanovesicles emulgel

The actual metformin HCl content of the formulation was found (98.7%).

In vivo study *Measurement of food intake and average body weight*

The amount of food intake decreased with metformin HCl treatment (Table 2), while the total percentage of weight gain showed a significant increase ($p < 0.0001$) in all groups compared to the normal group (group VI: 11.67% ± 12.21%), whereas only groups IV, V, and VI showed a significant decrease ($p < 0.0001$) compared to the control group (group I: 59.36% ± 13.23%) (Table 2).

Blood collection and biochemical assays

Despite being the mice treated topically, a valued systemic effect was noticed in the serum analysis results. Metformin HCl treatment showed no significant enhancement in TC levels (Table 3) in comparison with the control group (group I) (307.66 ± 25.09 mg/dl). On the other hand, TG decreased significantly ($p < 0.0001$) for both groups IV (124.17 ± 7.79 mg/dl) and V (121.93 ± 3.55 mg/dl) in addition to the normal group (VI) (72.95 ± 3.84 mg/dl) in comparison with the control group (I) (323.52 ± 39.80 mg/dl) (Table 3) with significant increase for groups I, II, and III compared to

Table 1. Rheology parameters of metformin HCl bilosomal emulgel at different shear rates and shear stresses.

Time interval (Second)	Shear rate(second^{-1})	Shear stress (Pa)	Torque %	Speed	Viscosity (Cp)
00:30	75.00	443.40 ± 20.45	22.60	10.00	591.20 ± 27.31
00:30	150.00	592.50 ± 7.06	30.20	20.00	395.00 ± 4.71
00:30	225.00	682.80 ± 1.95	34.80	30.00	303.50 ± 0.88
00:30	375.00	799.10 ± 3.01	41.20	50.00	212.20 ± 0.89
00:30	450.00	872.40 ± 4.07	44.50	60.00	193.90 ± 0.91
00:30	750.00	966.30 ± 6.40	51.02	100.00	89.01 ± 0.79
00:30	450.00	860.00 ± 6.86	43.80	60.00	191.10 ± 1.53
00:30	375.00	788.10 ± 4.05	40.20	50.00	210.20 ± 1.09
00:30	225.00	640.90 ± 5.72	32.70	30.00	284.90 ± 2.52
00:30	150.00	548.00 ± 4.56	27.90	20.00	365.40 ± 3.02
00:30	75.00	423.20 ± 5.66	21.60	10.00	564.20 ± 7.55

Values were expressed as mean ± SD, n = 3.

Table 2. Effect of metformin HCl bilosomal emulgel on the body weight, liver weight, and food intake of balb-c mice after 1 month of treatment.

Groups items	Control group (I)	Plain emulgel group (II)	Metformin HCl emulgel group (III)	Metformin HCl bilosomal emulgel (IV)	Metformin HCl bilosomal emulgel with penetration enhancer (V)	Normal group (VI)
Initial body weight (g)	25.31 ± 1.77	24.76 ± 2.41	24.29 ± 1.97	24.75 ± 2.44	25.54 ± 2.29	25.23 ± 1.75
Final body weight(g)	40.16 ± 0.87	39.35 ± 2.00	38.69 ± 2.33	33.55 ± 5.02	34.15 ± 4.05	28.04 ± 1.65
Body weight gain (g)	14.85 ± 2.32	14.59 ± 3.84	14.40 ± 2.87	8.79 ± 6.18	8.61 ± 4.78	2.81 ± 2.69
% of weight gain	59.36 ± 13.23[a]	60.58 ± 22.62[a]	60.08 ± 15.29[a]	36.95 ± 27.26[a,b]	34.59 ± 20.64[a,b]	11.67 ± 12.21[b]
Liver weight (g)	3.38 ± 9.01	3.77 ± 8.81	3.82 ± 6.93	2.44 ± 11.02	2.63 ± 0.56	1.95 ± 0.48
Average weekly food intake (g)	35.76 ± 5.36	36.33 ± 1.91	34.49 ± 3.04	29.46 ± 4.91	31.69 ± 4.89	29.19 ± 5.08

Values were expressed as mean ± SE, $n = 5$.
[a] has a significant difference at $p < 0.0001$, when compared with control model (Group I) values.
b has a significant difference at p < 0.0001, when compared with normal group (Group VI) values.

group VI (normal). HDL-c showed a significant increase for groups IV and V compared to the control group (Fig. 5).

LDL-c (Friedewald and Iranian) showed a significant decrease ($p < 0.0001$) for groups IV, V, and VI in comparison with the control group (group I). While only groups I, II, and III showed a significant increase compared with the normal group (group VI) (Table 3). On the other hand, VLDL-c showed no significance ($p > 0.0001$) compared with the control and normal groups. Increasing HDL-c level leads to an improvement in the AI and consequently in the CRI; this matches the results shown in Table 3. Briefly, the serum lipid profile data showed an overall enhancement after treatment with the cholate-based nanovesicles emulgel of metformin HCl (Fig. 5).

Fasting glucose level (mg/dl) showed a significant decrease ($p < 0.0001$) in groups IV, V, and VI compared to group I (control group) (Table 3). Fasting insulin level (uIU/ml) showed no significant change among all the groups ($p > 0.0001$) as clarified in Table 3.

ALT showed a normal range all over the groups (Table 4) (Hadizadeh *et al*., 2017). AST results showed a significant increase ($p < 0.0001$) for groups I, II, and III regarding the normal group (129.12 ± 6.60 U/l), while groups IV, V, and VI showed a significant decrease ($p < 0.0001$) in comparison to the control group (329.90 ± 19.06 U/l). Table 4 displays the calculated AST/ALT ratio of the results (Hadizadeh *et al*., 2017; Sporea *et al*., 2018). The results showed the significant lowering effect of metformin HCl cholate-based nanovesicles emulgel on the AST enzyme.

Groups I (control group), II, and III presented a significant increase ($p < 0.0001$) in serum TNF-α (1,297.56 ± 25.32 pg/ml) compared to the normal group (731.63 ± 9.58 pg/ml) (Table 4) that points to the incidence of NAFLD. On the other hand, the metformin HCl cholate-based nanovesicles emulgel with and without the addition of the penetration enhancer (DMS) showed a significant decrease ($p < 0.0001$) weighed against the control group, confirming the topical improvement effect of metformin HCl in treating NAFLD.

Hepatic weight and morphology

Histopathology of NAFLD infected liver usually shows numerous fat vacuoles with mild to moderate fibrosis (Nakamura and Terauchi, 2013; Nascimbeni *et al*., 2018; Santhekadur *et al*., 2018; Takahashi and Fukusato, 2014). Histopathological examination of the studied groups is elucidated in Figure 6a–f. Group I and II (control and plain emulgel groups) showed copious

Table 3. Effect of metformin HCl bilosomal emulgel on the blood sugar and lipid profile in balb-c mice after 1 month of treatment.

Groupsitems	Control group (I)	Plain emulgel group (II)	Metformin HCl emulgel group (III)	Metformin HCl bilosomal emulgel (IV)	Metformin HCl bilosomal emulgel with penetration enhancer (V)	Normal group (VI)
TC (mg/dl)	307.66 ± 25.09[b]	313.88 ± 34.73[b]	303.56 ± 50.53[b]	275.69 ± 26.50[b]	243.36 ± 22.58[b]	144.10 ± 13.65[a]
TG (mg/dl)	323.52 ± 39.80[b]	303.16 ± 38.48[b]	259.95 ± 30.05[b]	124.17 ± 7.79[a]	121.93 ± 3.55[a]	72.95 ± 3.84[a]
HDL (mg/dl)	101.72 ± 8.12	103.20 ± 7.61	111.29 ± 12.76	208.94 ± 37.01[a,b]	190.02 ± 18.91[a,b]	94.88 ± 3.70
LDL-c (Friedewald) (mg/dl)	141.23 ± 15.01[b]	150.05 ± 41.51[b]	140.28 ± 33.75[b]	41.91 ± 13.03[a]	28.96 ± 19.26[a]	34.63 ± 15.87[a]
LDL -c (Iranian) (mg/dl)	298.33 ± 35.68[b]	291.50 ± 38.59[b]	252.74 ± 46.44[b]	69.07 ± 10.05[a]	57.94 ± 15.09[a]	35.23 ± 14.68[a]
VLDL-c (mg/dl)	64.70 ± 7.96	60.63 ± 7.69	51.99 ± 6.01	24.83 ± 1.56	24.39 ± 0.71	14.59 ± 0.77
AI	2.06 ± 0.21	2.16 ± 0.51	1.69 ± 0.17	0.40 ± 0.13	0.30 ± 0.13	0.54 ± 0.19
CRI	3.06 ± 0.21	3.16 ± 0.51	2.69 ± 0.17	1.40 ± 0.13	1.30 ± 0.13	1.54 ± 0.19
Glucose (mg/dl)	203.98 ± 23.69[b]	186.62 ± 14.07[b]	163.45 ± 18.51	115.04 ± 9.44[a]	115.27 ± 6.73[a]	109.38 ± 8.40[a]
Insulin (uIU/ml)	13.92 ± 4.43	10.98 ± 3.99	9.81 ± 3.03	7.69 ± 1.75	7.96 ± 1.48	2.99 ± 0.25
HOMA-IR	7.99 ± 3.10	5.01 ± 1.79	4.48 ± 2.04	2.07 ± 0.39	2.26 ± 0.44	0.82 ± 0.13
QUICKI	0.31 ± 0.03	0.31 ± 0.01	0.32 ± 0.01	0.35 ± 0.01	0.34 ± 0.00	0.40 ± 0.01

Values were expressed as mean ± SE, $n = 5$.
TC, total cholesterol; TG, triglycerides; HDL, high-density lipoprotein; LDL-c, low-density lipoprotein cholesterol; VLDL-c, very low-density lipoprotein cholesterol; AI, atherogenic index; CRI, coronary risk index; HOMA-IR, homeostatic model assessment for insulin resistance; QUICKI, quantitative insulin sensitivity check index.
[a] has a significant difference at $p < 0.0001$, when compared with model control (Group I) values.
[b] has a significant difference at $p < 0.0001$, when compared with normal group (Group VI) values.

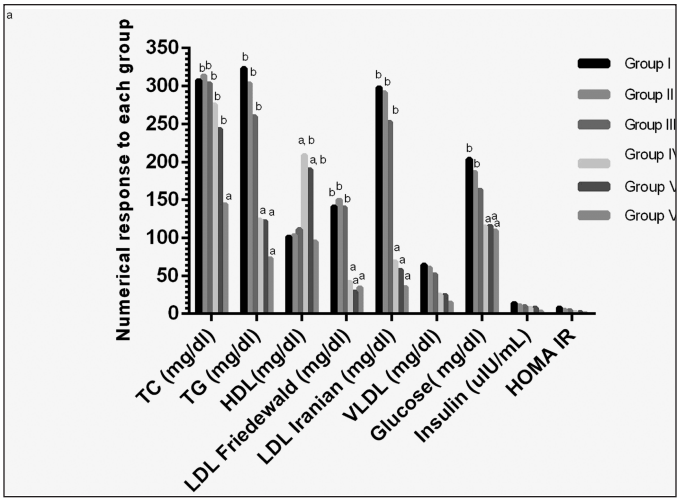

Figure 5. Two-way ANOVA of serum analysis for each mice group. a A significant difference at p < 0.0001 compared with model control (Group I) values. b A significant difference at p < 0.0001 compared with normal group (Group VI) values. TC, total cholesterol; TG, triglycerides; HDL, high-density lipoprotein; LDL-c, low-density lipoprotein cholesterol; VLDL-c, very low-density lipoprotein cholesterol; HOMA-IR, homeostatic model assessment for insulin resistance.

fat vacuoles with moderate fibrosis owed to NAFLD (Fig. 6a and b). Group I showed congestion of the hepatic blood vessels too. Group III (Fig. 6c) exhibits no enhancement in fat vacuoles or even fibrosis than the control group (group I).

On the other hand, the groups treated with metformin HCl cholate-based nanovesicles emulgel (IV and V) perceived a manifest diminution in the number of hepatic fat vacuoles alongside fibrosis enhancement (Fig. 6d and e). Still, it is hard to say that healthy cells are back to normal as those appearing in the normal group (VI) (Fig. 6f) which showed a healthy liver confirming the experimental model's validity.

DISCUSSION

Cholate-based vesicles are spherical, 5–200 nm in size, and can be uni- or multilamellar. In general, it consists of two layers; the inner layer consists of hydrophilic drugs and/or antigens, and the outer layer consists of bile salts (cholates) and/or hydrophobic drugs. Materials used in the formulation of its encompass are mainly nonionic surfactants and bile salts; lipids such as cholesterol are also included. It involves nonionic surfactants and exhibits a better quality of transdermal delivery than other nanovesicles (Al-Mahallawi *et al*., 2015). Bile salts produce extremely stable vesicles for transdermal distribution by acting as electrostatic stabilizers and edge activators with fluidizing effects (El Zaafarany *et al*., 2010). Bilosomes can be prepared by the solvent vaporization method (Al-Mahallawi *et al*., 2015).

TEM imaging of metformin HCl cholate-based nanovesicles fortified its successful nanospherical configuration (64.85 ± 7.14 nm as clarified in (Fig. 2).

A zeta potential of −40 ± 5.54 mV (Fig. 3) reflects the vesicle's stability as zeta potential > ± 30 mV; zeta potential value around ±30 mV designates the vesicle's electric repulsion and pleasant stability with no aggregation upon storage (Badria and Mazyed, 2020). The bile salt content of the formulation may cause the resulting negative charge due to its anionic nature and strongly acidic taurine group, which can enhance the cholate-based nanovesicles skin permeation (Chen-yu *et al*., 2012).

The clarity, homogeneity, and pH of the prepared cholate-based nanovesicles emulgel of metformin HCl declares its safety for skin application with no prediction of irritation,

Table 4. Effect of metformin HCl bilosomal emulgel on the liver enzymes and TNF alpha in Balb-C mice after 1 month of treatment.

Groupsitems	Control group (I)	Plain emulgel group (II)	Metformin HCl emulgel group (III)	Metformin HCl bilosomal emulgel (IV)	Metformin HCl bilosomal emulgel with penetration enhancer (V)	Normal group (VI)
AST (U/l)	329.90 ± 19.06[b]	276.69 ± 36.10[b]	231.79 ± 2.24[b]	173.69 ± 8.13[a]	169.08 ± 10.53[a]	61.12 ± 4.54[a]
ALT (U/l)	81.79 ± 5.81	83.09 ± 5.27	69.78 ± 9.34	47.98 ± 3.77	47.49 ± 4.59	44.29 ± 2.64
AST/ALT	4.14 ± 0.44	3.33 ± 0.35	3.49 ± 0.38	3.67 ± 0.18	3.75 ± 0.54	1.39 ± 0.12
TNF alpha (pg/ml)	1,297.56 ± 25.32[b]	1,293.05 ± 21.82[b]	1,207.68 ± 62.67[b]	780.73 ± 32.25 [a]	769.35 ± 32.86[a]	731.63 ± 9.58[a]

AST, aspartate aminotransferase; ALT, alanine aminotransferase; and TNF alpha, tumor necrosis factor.Values were expressed as mean ± SE, $n = 5$.
[a] has a significant difference at $p < 0.0001$, when compared with model control (Group I) values.
[b] has a significant difference at $p < 0.0001$, when compared with normal group (Group VI) values.

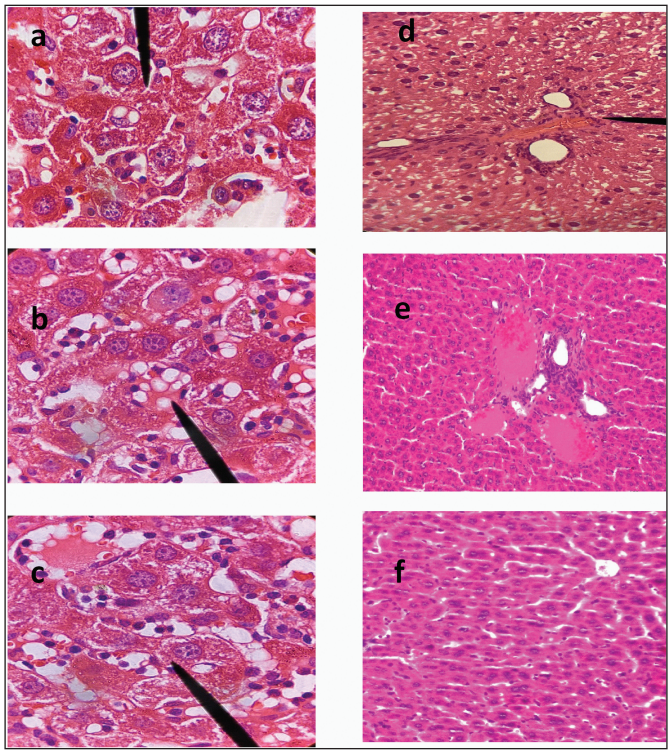

Figure 6. Histology micrograph of liver tissue; hematoxylin and eosin (magnification × 100). (a) group I (control group); (b) group II (plain emulgel treated); (c) group III (metformin HCl emulgel treated); (d) group IV (metformin HCl cholate-based nanovesicles emulgel treated); (e) group V (metformin HCl cholate-based nanovesicles emulgel including penetration enhancer treated); (f) group VI (normal group).

whereas highly basic or acidic pH application on the skin may cause extreme irritation, dryness, or even erythema (El-Menshawe *et al*., 2018; El-Ridy *et al*., 2018; Mohamed *et al*., 2019).

The rheological conduct of a semisolid pharmaceutical preparation is crucial for its quality control (Seoane-Viaño *et al*., 2021). It indicates the possible physical or chemical changes during and after the formulation process. Figure 4a and b shows shear thinning behavior ($N < 1$) that increases the skin absorption area giving a good spreadability to the emulgel (Dhawan *et al*., 2014; Mohamed *et al*., 2019). The negligible hysteresis loop area signposted the emulgel rapid recovery after eliminating the shear rate (Gupta *et al*., 2012; Mohamed *et al*., 2019).

The large diameter in spreadability determination exhibits better skin absorption on a larger skin area (Dhawan *et al*., 2014). The extrusion conduct of an emulgel formulation is a worthy feature for patient acceptance and application duration. The results verified the appropriateness of the developed formulation for topical application. The formulation drug content (98.7%) meets the terms of the official necessities (90% to 110% of the label claim) (Martins and Farinha, 1998).

NAFLD can be defined as steatosis of the liver deprived of liver injuries, such as inflating the hepatocytes or fibrosis. It is described as a disorder where >5% of hepatocytes show macroscopic steatosis under light microscopy in the privation of other causes of liver impairment (Byrne, 2010). It is diagnosed by the appearance of liver fat vacuoles, as recognized by imaging or histology, in the lack of triggering factors of liver fat deposition. Hepatic steatosis, inflammation, and liver cell destruction (swelling) with or without fibrosis are all symptoms of NASH (Valls *et al*., 2006). NAFLD is more dominant in males than females for unidentified explanations (DiStefano, 2020).

TNF-α partakes in NAFLD progress as it wields many proinflammatory possessions and prompts pathogenic pathways. TNF-α upsurges the serum TG, lowers the HDL-c, and raises cholesterogenic gene expression by suppressing cholesterol elimination (Tangvarasittichai *et al*., 2016). Furthermore, TNF-α may correspondingly endorse hepatocyte death aiding in the pathophysiology of hepatic fibrosis (Zhang *et al*., 2013).

Metformin's HCl role in NAFLD treatment has been examined in numerous recent studies, many of which focused on the liver's histology and liver enzymes besides its role in decreasing glucose production in the liver (Hundal *et al*., 2000, Li *et al*., 2013; Viollet and Foretz, 2013). Furthermore, metformin HCl suppresses TNF-α (Hammad *et al*., 2021) which was noticeably elevated in NAFLD and worsened it (Ajmal *et al*., 2014; Yang and Seki, 2015). In addition, its augmenting effect plummeted the crucial risk factors for NAFLD (obesity and insulin resistance) (Hundal and Inzucchi, 2003).

The amount of food intake decreased with metformin HCl treatment (Table 2) due to its known effect on decreasing food appetite (Kim *et al*., 2016; Lv *et al*., 2012; Matsui *et al*., 2010). Concerning balb-c mice, the change in body weight is generally negligible; it is so-called the obesity-resistant strain (Farrell *et al*., 2014; Kim *et al*., 2011; Nishikawa *et al*., 2007). Despite that, the total percentage of weight gain showed a significant decrease ($p <$ 0.0001) compared to the control (Table 2).

Despite being the mice treated topically, a valued systemic effect was noticed in the serum analysis results. That can be attributed to the cholate-based nanovesicles nanosize, ultraflexibility (Aziz *et al*., 2019), and flash permeation ability (Aziz *et al*., 2019; Salem *et al*., 2022) even without using a permeation enhancer that came besides its liver targeting characteristics (El-Nabarawi *et al*., 2021).

TG decreased significantly as metformin HCl affected the TG mainly with a negligible effect on the TC (Sin *et al*., 2011; Wulffele *et al*., 2004; Xu *et al*., 2015); also it enhances the lipid profile by increasing HDL-C and decreasing LDL-C and VLDL (Alkuraishy and Al-Gareeb, 2015; Ghatak *et al*., 2011). The results agreed with this indicating the enhancing effect of metformin HCl cholate-based nanovesicles emulgel on HDL-c (Fig. 5).

Increasing HDL-c level leads to an improvement in the AI and consequently in the CRI, matching the results shown in Table 3. Briefly, the serum lipid profile data showed an overall enhancement after treatment with the cholate-based nanovesicles emulgel of metformin HCl (Fig. 5).Insulin resistance is also a crucial sign of NAFLD, as it leads to abandoned liver production of glucose and lessened glucose uptake (Muoio and Newgard, 2008). Accordingly, the determination of glucose, insulin, HOMA-IR, and QUICKI helps in NAFLD assessment (Motamed *et al*., 2016). Metformin HCl lowers the glucose level by decreasing its intestinal absorption (Viollet and Foretz, 2013), increasing its uptake from the blood into the tissues and decreasing its production from the liver (Hundal *et al*., 2000; Viollet and Foretz, 2013). Metformin also affects the insulin requirements for glucose discarding (increasing insulin sensitivity) without affecting the serum insulin levels (Gaggini *et al*., 2013; Hadizadeh *et al*., 2017).

The optimal limit point (the cut-off point) for HOMA-IR in the NAFLD diagnosis is >1.79, while for QUICKI, it is <0.347 (Salgado *et al*., 2010). Generally, a higher value of HOMA-IR and a lower value of QUICKI increase the insulin resistance risk (Motamed *et al*., 2016). HOMA-IR and QUICKI results revealed the metformin HCl enhancement effect on NAFLD by increasing insulin sensitivity (Hosono *et al*., 2010) as clarified in Table 3.

ALT and AST results are shown (Table 4 was as predicted, as a marked elevation in ALT level is not common in NAFLD but is mainly associated with liver steatosis (Hadizadeh *et al*., 2017; Pearce *et al*., 2013). AST elevation can be used as an independent marker for NAFLD, mainly when the values are twice the normal levels (Hadizadeh *et al*., 2017). Recently, AST/ALT ratio became used for NAFLD diagnosis; the more of this ratio (>1.5), the more possibility of having fatty liver disease (Hadizadeh *et al*., 2017; Sporea *et al*., 2018). AST/ALT ratio confirms the formulation's influential role in enhancing NAFLD.

TNF-α, with its proinflammatory effect, plays a pivotal role in NAFLD progression (Hadizadeh *et al*., 2017; Jovinge *et al*., 1998) through different mechanisms as it increases the serum levels of TG (Jovinge *et al*., 1998) and decreases the HDL-c levels and insulin sensitivity (Tacer *et al*., 2007). Besides that, TNF induces apoptosis and proliferation in hepatic cells leading to liver fibrosis (Galle, 1997; Yang and Seki, 2015). Elevated serum levels of TNF-α can be related to NAFLD, and normalization of its results enhances insulin sensitivity and NAFLD (Ajmal *et al*., 2014; Hadizadeh *et al*., 2017). The decreasing effect of the prepared metformin emulgel on the TNF-α confirms the topical improvement effect of metformin HCl in treating NAFLD.

Nevertheless, the difference in liver weight among the groups was insignificant ($p > 0.0001$) (Table 2), and metformin HCl cholate-based nanovesicles emulgel treated groups parades an acceptable reduction in the liver weight put side by side with the control group. Histopathology of NAFLD-infected liver usually shows numerous fat vacuoles with mild to moderate fibrosis (Nakamura and Terauchi, 2013; Nascimbeni *et al*., 2018; Santhekadur *et al*., 2018; Takahashi and Fukusato, 2014). Histopathological examination of the studied groups is elucidated in Figure 6a–f revealing the therapeutic effect of metformin HCl cholate-based nanovesicles emulgel in the topical treatment of NAFLD and signifying the success of liver targeting by metformin HCl cholate-based bile salts (El-Nabarawi *et al*., 2021).

CONCLUSION

A cholate-based nanovesicles emulgel of metformin HCl was fruitfully prepared and assessed to open a new gateway to use metformin HCl in the transdermal treatment of NAFLD. The TEM imaging verified a successful formulation of nano cholate-based bile salts, and its stability was confirmed by the zeta potential result and then incorporated into an emulgel. Furthermore, the prepared cholate-based nanovesicles emulgel showed suitable clarity, homogeneity, pH, spreadability, extrudability, and drug content. In addition, the rheology behavior was perfect thixotropic as demanded by a transdermal formulation. Furthermore, the *in vivo* study on balb-c mice showed impressive results in treating NAFLD transdermally. The overall consequences of these findings highlight the cholate-based nanovesicles emulgel as a promising formulation for acceptable level of transdermal treatment of NAFLD.

STATISTICAL ANALYSIS

The significance of differences was ascertained by a two-way analysis of variance (ANOVA) using Graph Pad Prism edition 6.0 for Windows, Graph Pad Software (San Diego, CA). The results were stated in mean ± SE, and p-value < 0.0001 was deemed statistically significant.

ACKNOWLEDGMENTS

The authors are grateful for Nahda University in Beni Suef Central Lab for providing the amenities to elicit this work.

AUTHOR CONTRIBUTIONS

All authors made substantial contributions to conception and design, acquisition of data, or analysis and interpretation of data; took part in drafting the article or revising it critically for important intellectual content; agreed to submit to the current journal; gave final approval of the version to be published; and agree to be accountable for all aspects of the work. All the authors are eligible to be an author as per the international committee of medical journal editors (ICMJE) requirements/guidelines.

FINANCIAL SUPPORT

There is no funding to report.

CONFLICTS OF INTERESTS

The authors report no conflicts of interest.

ETHICAL APPROVALS

The *in vivo* study protocol was done as stated by the guidelines consented by the Pharmacology and Toxicology Department, Faculty of Pharmacy at Beni Suef University, Egypt. In addition, it was based on the National Institutes of Health Guide for Care and Use of Laboratory Animals recommendations. The animal protocol was approved by BSU-IACUC reviewers with approval number 022–351.

DATA AVAILABILITY

All data generated and analyzed are included in this research article.

PUBLISHER'S NOTE

This journal remains neutral with regard to jurisdictional claims in published institutional affiliation.

REFERENCES

Abdallah MH, Lila ASA, Unissa R, Elsewedy HS, Elghamry HA, Soliman MS. Preparation, characterization and evaluation of anti-inflammatory and anti-nociceptive effects of brucine-loaded nanoemulgel. Colloids Surf B Biointerfaces, 2021; 205:111868.

Ahmed S, Kassem MA, Sayed S. Bilosomes as promising nanovesicular carriers for improved transdermal delivery: construction, in vitro optimization, ex vivo permeation and in vivo evaluation. Int J Nanomed, 2020; 15:9783.

Ajmal MR, Yaccha M, Malik MA, Rabbani M, Ahmad I, Isalm N, Abdali N. Prevalence of nonalcoholic fatty liver disease (NAFLD) in patients of cardiovascular diseases and its association with hs-CRP and TNF-α. Indian Heart J, 2014; 66:574–9.

Albash R, El-Nabarawi MA, Refai H, Abdelbary AA. Tailoring of PEGylated bilosomes for promoting the transdermal delivery of olmesartan medoxomil: in-vitro characterization, ex-vivo permeation and in-vivo assessment. Int J Nanomed, 2019; 14:6555.

Alexander A, Khichariya A, Gupta S, Patel RJ, Giri TK, Tripathi DK. Recent expansions in an emergent novel drug delivery technology: emulgel. J Control Release, 2013; 171:122–32.

Alkuraishy HM, Al-Gareeb AI. New insights into the role of metformin effects on serum omentin-1 levels in acute myocardial infarction: cross-sectional study. Emerg Med Int, 2015; 2015:283021.

Al-Mahallawi AM, Abdelbary AA, Aburahma MH. Investigating the potential of employing bilosomes as a novel vesicular carrier for transdermal delivery of tenoxicam. Int J Pharm, 2015; 485:329–40.

Aziz DE, Abdelbary AA, Elassasy AI. Investigating superiority of novel bilosomes over niosomes in the transdermal delivery of diacerein: in vitro characterization, ex vivo permeation and in vivo skin deposition study. J Liposome Res, 2019; 29:73–85.

Badria F, Mazyed E. Formulation of nanospanlastics as a promising approach for improving the topical delivery of a natural leukotriene inhibitor (3-Acetyl-11-Keto-β-Boswellic Acid): statistical optimization, *in vitro* characterization, and *ex vivo* permeation study. Drug Design Dev Ther, 2020; 14:3697.

Basak SC, Kumar KS, Ramalingam M. Design and release characteristics of sustained release tablet containing metformin HCl. Rev Bras Ciênc Farm, 2008; 44:477–83.

Basak S, Rahman J, Ramalingam M. Design and in vitro testing of a floatable gastroretentive tablet of metformin hydrochloride. Int J Pharm Sci, 2007; 62:145–8.

Bellentani S, Scaglioni F, Marino M, Bedogni G. Epidemiology of non-alcoholic fatty liver disease. Dig Dis, 2010; 28:155–61.

Byrne CD. Fatty liver: role of inflammation and fatty acid nutrition. Prostaglandins Leukot Essent Fatty Acids (PLEFA), 2010; 82:265–71.

Chen-Yu G, Chun-Fen Y, Qi-Lu L, Qi T, Yan-Wei X, Wei-Na L, Guang-Xi Z. Development of a quercetin-loaded nanostructured lipid carrier formulation for topical delivery. Int J Pharm, 2012; 430:292–8.

Cicero AF, Tartagni E, Ertek S. Metformin and its clinical use: new insights for an old drug in clinical practice. Arch Med Sci AMS, 2012; 8:907.

Cutfield WS, Jefferies CA, Jackson WE, Robinson EM, Hofman PL. Evaluation of HOMA and QUICKI as measures of insulin sensitivity in prepubertal children. Pediatr Diabetes, 2003; 4:119–25.

Dhawan B, Aggarwal G, Harikumar S. Enhanced transdermal permeability of piroxicam through novel nanoemulgel formulation. Int J Pharm Investig, 2014; 4:65.

Distefano JK. NAFLD and NASH in postmenopausal women: implications for diagnosis and treatment. Endocrinology, 2020; 161:bqaa134.

El-Menshawe SF, Ali AA, Rabeh MA, Khalil NM. Nanosized soy phytosome-based thermogel as topical anti-obesity formulation: an approach for acceptable level of evidence of an effective novel herbal weight loss product. Int J Nanomed, 2018; 13:307.

El-Nabarawi M, Nafady M, Elmenshawe S, Elkarmalawy M, Teaima M. Liver targeting of daclatasvir via tailoring sterically stabilized bilosomes: fabrication, comparative in vitro/in vivo appraisal and biodistribution studies. Int J Nanomed, 2021; 16:6413.

El-Ridy MS, Yehia SA, Mohsen AM, El-Awdan SA, Darwish AB. Formulation of niosomal gel for enhanced transdermal lornoxicam delivery: in-vitro and in-vivo evaluation. Curr Drug Deliv, 2018; 15:122–33.

El Zaafarany GM, Awad GA, Holayel SM, Mortada ND. Role of edge activators and surface charge in developing ultradeformable vesicles with enhanced skin delivery. Int J Pharm, 2010; 397:164–72.

Farrell GC, Mridha AR, Yeh MM, Arsov T, Van Rooyen DM, Brooling J, Nguyen T, Heydet D, Delghingaro-Augusto V, Nolan CJ. Strain dependence of diet-induced NASH and liver fibrosis in obese mice is linked to diabetes and inflammatory phenotype. Liver Int, 2014; 34:1084–93.

Gaggini M, Morelli M, Buzzigoli E, Defronzo RA, Bugianesi E, Gastaldelli A. Non-alcoholic fatty liver disease (NAFLD) and its connection with insulin resistance, dyslipidemia, atherosclerosis and coronary heart disease. Nutrients, 2013; 5:1544–60.

Galle PR. Apoptosis in liver disease. J Hepatol, 1997; 27:405–12.

Ghatak SB, Dhamecha PS, Bhadada SV, Panchal SJ. Investigation of the potential effects of metformin on atherothrombotic risk factors in hyperlipidemic rats. Eur J Pharmacol, 2011; 659:213–23.

Green CJ, Marjot T, Tomlinson JW, Hodson L. Of mice and men: is there a future for metformin in the treatment of hepatic steatosis? Diabetes Obes Metab, 2019; 21:749–60.

Gupta A, Aggarwal G, Singla S, Arora R. Transfersomes: a novel vesicular carrier for enhanced transdermal delivery of sertraline: development, characterization, and performance evaluation. Sci Pharm, 2012; 80:1061–80.

Hadizadeh F, Faghihimani E, Adibi P. Nonalcoholic fatty liver disease: diagnostic biomarkers. World J Gastrointest Pathophysiol, 2017; 8:11.

Hammad AM, Ibrahim YA, Khdair SI, Hall FS, Alfaraj M, Jarrar Y, Abed AF. Metformin reduces oxandrolone-induced depression-like behavior in rats via modulating the expression of IL-1β, IL-6, IL-10 and TNF-α. Behav Brain Res, 2021; 414:113475.

Harrison SA, Torgerson S, Hayashi PH. The natural history of nonalcoholic fatty liver disease: a clinical histopathological study. Am J Gastroenterol, 2003; 98:2042–7.

Hosono K, Endo H, Takahashi H, Sugiyama M, Uchiyama T, Suzuki K, Nozaki Y, Yoneda K, Fujita K, Yoneda M. Metformin suppresses azoxymethane-induced colorectal aberrant crypt foci by activating AMP-activated protein kinase. Mol Carcinog, 2010; 49:662–71.

Hundal RS, Inzucchi SE. Metformin. Drugs, 2003; 63:1879–94.

Hundal RS, Krssak M, Dufour S, Laurent D, Lebon V, Chandramouli V, Inzucchi SE, Schumann WC, Petersen KF, Landau BR. Mechanism by which metformin reduces glucose production in type 2 diabetes. Diabetes, 2000; 49:2063–9.

Jain SK, Gupta A. Development of gelucire 43/01 beads of metformin hydrochloride for floating delivery. AAPS PharmSciTech, 2009; 10:1128–36.

Jovinge S, Hamsten A, Tornvall P, Proudler A, Båvenholm P, Ericsson CG, Godsland I, De Faire U, Nilsson J. Evidence for a role of tumor necrosis factor α in disturbances of triglyceride and glucose metabolism predisposing to coronary heart disease. Metabolism, 1998; 47:113–8.

Kim EJ, Choi MR, Park H, Kim M, Hong JE, Lee JY, Chun HS, Le KW, Yoon Park JH. Dietary fat increases solid tumor growth and metastasis of 4T1 murine mammary carcinoma cells and mortality in obesity-resistant BALB/c mice. Breast Cancer Res, 2011; 13:1–13.

Kim HJ, Jin BY, Oh MJ, Shin KH, Choi SH, Kim DH. The effect of metformin on neuronal activity in the appetite-regulating brain regions of mice fed a high-fat diet during an anorectic period. Physiol Behav, 2016; 154:184–90.

Kwon CS, Sohn HY, Kim SH, Kim JH, Son KH, Lee JS, Lim JK, Kim JS. Anti-obesity effect of *Dioscorea* nipponica Makino with lipase-inhibitory activity in rodents. Biosci Biotechnol Biochem, 2003; 67:1451–6.

Li Y, Liu L, Wang B, Wang J, Chen D. Metformin in non-alcoholic fatty liver disease: a systematic review and meta-analysis. Biomed Rep, 2013; 1:57–64.

Lv WS, Wen JP, Li L, Sun RX, Wang J, Xian YX, Cao CX, Wang YL, Gao YY. The effect of metformin on food intake and its potential role in hypothalamic regulation in obese diabetic rats. Brain Res, 2012; 1444:11–9.

Majid H, Masood Q, Khan AH. Homeostatic model assessment for insulin resistance (HOMA-IR): a better marker for evaluating insulin resistance than fasting insulin in women with polycystic ovarian syndrome. J Coll Physicians Surg Pak, 2017; 27:123–6.

Martins JM, Farinha A. Uniformity of dosage units—comparative study of methods and specifications between Eur. Pharm. 3rd and USP 23. J Pharm Biomed Anal, 1998; 18:487–95.

Matsui Y, Hirasawa Y, Sugiura T, Toyoshi T, Kyuki K, Ito M. Metformin reduces body weight gain and improves glucose intolerance in high-fat diet-fed C57BL/6J mice. Biol Pharm Bull, 2010; 33:963–70.

Mohamed MI, Abdelbary AA, Kandil SM, Mahmoud TM. Preparation and evaluation of optimized zolmitriptan niosomal emulgel. Drug Dev Ind Pharm, 2019; 45:1157–67.

Motamed N, Miresmail SJH, Rabiee B, Keyvani H, Farahani B, Maadi M, Zamani F. Optimal cutoff points for HOMA-IR and QUICKI in the diagnosis of metabolic syndrome and non-alcoholic fatty liver disease: a population based study. J Diabetes Complicat, 2016; 30:269–74.

Muoio DM, Newgard CB. Molecular and metabolic mechanisms of insulin resistance and β-cell failure in type 2 diabetes. Nat Rev Mol Cell Biol, 2008; 9:193–205.

Nakamura A, Terauchi Y. Lessons from mouse models of high-fat diet-induced NAFLD. Int J Mol Sci, 2013; 14:21240–57.

Nascimbeni F, Ballestri S, Machado MV, Mantovani A, Cortez-Pinto H, Targher G, Lonardo A. Clinical relevance of liver histopathology and different histological classifications of NASH in adults. Expert Rev Gastroenterol Hepatol, 2018; 12:351–67.

Nauck M, Warnick GR, Rifai N. Methods for measurement of LDL-cholesterol: a critical assessment of direct measurement by homogeneous assays versus calculation. Clin Chem, 2002; 48:236–54.

Neuman MG, Cohen LB, Nanau RM. Biomarkers in nonalcoholic fatty liver disease. Can J Gastroenterol Hepatol, 2014; 28:607–18.

Ng LC, Gupta M. Transdermal drug delivery systems in diabetes management: a review. Asian J Pharm Sci, 2020; 15:13–25.

Nishikawa S, Yasoshima A, Doi K, Nakayama H, Uetsuka K. Involvement of sex, strain and age factors in high fat diet-induced obesity in C57BL/6J and BALB/cA mice. Exp Anim, 2007; 56:263–72.

Obika M, Noguchi H. Diagnosis and evaluation of nonalcoholic fatty liver disease. Exp Diabetes Res, 2011; 2012:145754; doi: 10.1155/2012/145754.

Pearce SG, Thosani NC, Pan JJ. Noninvasive biomarkers for the diagnosis of steatohepatitis and advanced fibrosis in NAFLD. Biomarker Res, 2013; 1:1–11.

Picchi MG, Mattos AMD, Barbosa MR, Duarte CP, Gandini MDA, Portari GV, Jordão AA. A high-fat diet as a model of fatty liver disease in rats. Acta Cir Bras, 2011; 26:25–30.

Popescu LA, Virgolici B, Lixandru D, Miricescu D, Condruţ E, Timnea O, Ranetti A, Militaru M, Mohora M, Zăgrean L. Effect of diet and omega-3 fatty acids in NAFLD. Rom J Morphol Embryol, 2013; 54:785–90.

Rahmadi M, Nurhan AD, Pratiwi ED, Prameswari DA, Panggono SM, Nisak K, Khotib J. The effect of various high-fat diet on liver histology in the development of NAFLD models in mice. J Basic Clin Physiol Pharmacol, 2021; 32:547–53.

Salem HF, Kharshoum RM, Awad SM, Mostafa MA, Abou-Taleb HA. Tailoring of retinyl palmitate-based ethosomal hydrogel as a novel nanoplatform for acne vulgaris management: fabrication, optimization, and clinical evaluation employing a split-face comparative study. Int J Nanomed, 2021; 16:4251.

Salem HF, Nafady MM, Ali AA, Khalil NM, Elsisi AA. Evaluation of metformin hydrochloride tailoring bilosomes as an effective transdermal nanocarrier. Int J Nanomed, 2022; 17:1185.

Salgado ALFDA, Carvalho LD, Oliveira AC, Santos VND, Vieira JG, Parise ER. Insulin resistance index (HOMA-IR) in the differentiation of patients with non-alcoholic fatty liver disease and healthy individuals. Arq Gastroenterol, 2010; 47:165–9.

Santhekadur PK, Kumar DP, Sanyal AJ. Preclinical models of non-alcoholic fatty liver disease. J Hepatol, 2018; 68:230–7.

Seoane-Viaño I, Januskaite P, Alvarez-Lorenzo C, Basit AW, Goyanes A. Semi-solid extrusion 3D printing in drug delivery and biomedicine: personalised solutions for healthcare challenges. J Control Release, 2021; 332:367–89.

Sin HY, Kim JY, Jung KH. Total cholesterol, high density lipoprotein and triglyceride for cardiovascular disease in elderly patients treated with metformin. Arch Pharm Res, 2011; 34:99–107.

Sporea I, Popescu A, Dumitraşcu D, Brisc C, Nedelcu L, Trifan A, Gheorghe L, Braticevici CF. Nonalcoholic fatty liver disease: status quo. J Gastrointestin Liver Dis, 2018; 27(4):439–48.

Tacer KF, Kuzman D, Seliskar M, Pompon D, Rozman D. TNF-α interferes with lipid homeostasis and activates acute and proatherogenic processes. Physiol Genom, 2007; 31:216–27.

Tag HM. Hepatoprotective effect of mulberry (*Morus nigra*) leaves extract against methotrexate induced hepatotoxicity in male albino rat. BMC complement Altern Med, 2015; 15:1–9.

Takahashi Y, Fukusato T. Histopathology of nonalcoholic fatty liver disease/nonalcoholic steatohepatitis. World J Gastroenterol WJG, 2014; 20:15539.

Tan S, Gao B, Tao Y, Guo J, Su ZQ. Antiobese effects of capsaicin–chitosan microsphere (CCMS) in obese rats induced by high fat diet. J Agric Food Chem, 2014; 62:1866–74.

Tangvarasittichai S, Pongthaisong S, Tangvarasittichai O. Tumor necrosis factor-A, interleukin-6, C-reactive protein levels and insulin resistance associated with type 2 diabetes in abdominal obesity women. Indian J Clin Biochem, 2016; 31:68–74.

Valls C, Iannacconne R, Alba E, Murakami T, Hori M, Passariello R, Vilgrain V. Fat in the liver: diagnosis and characterization. Eur Radiol, 2006; 16:2292–308.

Vani YB, Haranath C, Reddy CSP, Bhargav E. Formulation and in vitro evaluation of piroxicam emulgel. Int J Pharm Sci Drug Res, 2018; 10:227–32.

Viollet B, Foretz M. Revisiting the mechanisms of metformin action in the liver. Ann Endocrinol, 2013; 74(2):123–9.

Wu J, Liu W, Xue C, Zhou S, Lan F, Bi L, Xu H, Yang X, Zeng FD. Toxicity and penetration of TiO2 nanoparticles in hairless mice and porcine skin after subchronic dermal exposure. Toxicol Lett, 2009; 191:1–8.

Wulffele EM, Kooy A, De Zeeuw D, Stehouwer C, Gansevoort R. The effect of metformin on blood pressure, plasma cholesterol and triglycerides in type 2 diabetes mellitus: a systematic review. J Intern Med, 2004; 256:1–14.

Xie F, Jia L, Lin M, Shi Y, Yin J, Liu Y, Chen D, Meng Q. ASPP 2 attenuates triglycerides to protect against hepatocyte injury by reducing autophagy in a cell and mouse model of non-alcoholic fatty liver disease. J Cell Mol Med, 2015; 19:155–64.

Xu T, Brandmaier S, Messias AC, Herder C, Draisma HH, Demirkan A, Yu Z, Ried JS, Haller T, Heier M. Effects of metformin on metabolite profiles and LDL cholesterol in patients with type 2 diabetes. Diabetes Care, 2015; 38:1858–67.

Yang YM, Seki E. TNFα in liver fibrosis. Curr Pathobiol Rep, 2015; 3:253–61.

Zhang Y, Zhang Y, Xie Y, Gao Y, Ma J, Yuan J, Li J, Wang J, Li L, Zhang J. Multitargeted inhibition of hepatic fibrosis in chronic iron-overloaded mice by *Salvia miltiorrhiza*. J Ethnopharmacol, 2013; 148:671–81.

How to cite this article:
Salem HF, Nafady MM, Ali AA, Khalil NM, Elsisi AA. Cholate-based nano emulgel of 1,1-dimethylbiguanide can diminish the liver damage in NAFLD induced by high-fat diet. J Appl Pharm Sci, 2023; 13(07):258–269.